MODELLING UHF ANTENNA COUPLING ON AIRCRAFT

Richard Evans Koehler

NAVAL POSTGRADUATE SCHOOL
Monterey, California

THESIS

MODELLING UHF ANTENNA COUPLING ON AIRCRAFT

by

Richard Evans Koehler

March 1975

Thesis Advisor: Stephen Jauregui
Co-Advisor: J. W. Adler

Approved for public release; distribution unlimited.

REPORT DOCUMENTATION PAGE

READ INSTRUCTIONS BEFORE COMPLETING FORM

1. REPORT NUMBER	2. GOVT ACCESSION NO. / 3. RECIPIENT'S CATALOG NUMBER
4. TITLE (and Subtitle): Modelling UHF Antenna Coupling on Aircraft	5. TYPE OF REPORT & PERIOD COVERED: Master's Thesis; March 1975
	6. PERFORMING ORG. REPORT NUMBER
7. AUTHOR(s): Richard Evans Koehler	8. CONTRACT OR GRANT NUMBER(s)
9. PERFORMING ORGANIZATION NAME AND ADDRESS: Naval Postgraduate School, Monterey, California 93940	10. PROGRAM ELEMENT, PROJECT, TASK AREA & WORK UNIT NUMBERS
11. CONTROLLING OFFICE NAME AND ADDRESS: Naval Postgraduate School, Monterey, California 93940	12. REPORT DATE: March 1975 / 13. NUMBER OF PAGES
14. MONITORING AGENCY NAME & ADDRESS (if different from Controlling Office): Naval Postgraduate School, Monterey, California 93940	15. SECURITY CLASS. (of this report): Unclassified / 15a. DECLASSIFICATION/DOWNGRADING SCHEDULE

16. DISTRIBUTION STATEMENT (of this Report)

Approved for public release; distribution unlimited.

17. DISTRIBUTION STATEMENT (of the abstract entered in Block 20, if different from Report)

18. SUPPLEMENTARY NOTES

19. KEY WORDS (Continue on reverse side if necessary and identify by block number)

On-Aircraft Antennas
Antenna Modelling Program
UHF Antennas
Antenna Coupling
Radiation Patterns
Roll Plane
Geometric Theory of Diffraction
Quarter Wave Antennas
Ground Plane Analysis

20. ABSTRACT (Continue on reverse side if necessary and identify by block number)

Antenna coupling is of particular interest on aircraft where the structure interacts with the antenna arrays. These arrays may be extremely complex as new electronic countermeasures and signal intelligence systems are added to aircraft.

The thesis attempts to find a method to predict such antenna interactions. Four general computer programs for antenna design

and radiation pattern determination are investigated and deficiencies and strengths noted. These programs primarily employ the moment method or geometrical theory of diffraction. Some interesting correlations are presented and recommendations on future potentially fruitful approaches are discussed.

Modelling UHF Antenna Coupling on Aircraft

by

Richard Evans Koehler
Lieutenant, United States Navy
B.S., Aeronautical Engineering, Purdue University, 1968

Submitted in partial fulfillment of the
requirements for the degree of

MASTER OF SCIENCE IN AERONAUTICAL ENGINEERING

from the

NAVAL POSTGRADUATE SCHOOL
March 1975

ABSTRACT

Antenna coupling is of particular interest on aircraft where the structure interacts with the antenna arrays. These arrays may be extremely complex as new electronic countermeasures and signal intelligence systems are added to aircraft.

The thesis attempts to find a method to predict such antenna interactions. Four general computer programs for antenna design and radiation pattern determination are investigated and deficiencies and strengths noted. These programs primarily employ the moment method or geometrical theory of diffraction. Some interesting correlations are presented and recommendations on future potentially fruitful approaches are discussed.

TABLE OF CONTENTS

LIST OF TABLES

LIST OF FIGURES

ACKNOWLEDGEMENTS

The author is indebted to a multitude of persons for their assistance and patience during the preparation of this thesis. I wish to thank Dr. Stephen Jauregui for guidance in selection of this thesis and the many contacts he provided to expand my knowledge of the subject area. I wish also to thank Dr. Richard W. Adler, under whose supervision I worked.

External to the Naval Postgraduate School, I received assistance from Keith Struckman of Sanders Associates in brass modelling, Bob Lee, Robert Hays and Joe Miller of NADC in BENT/ROLL application, Dr. J. Rockway in AMP application, and Dr. Robert Tanner of TCI in general moment methods applications.

I. INTRODUCTION

A. NEED FOR STUDY

Since the days of Operation Shoehorn in the early Viet Nam War era, airborne electronic warfare has experienced an explosive increase in platforms and complexity. All tactical and strategic U.S. aircraft are now equipped with various electronic countermeasures systems providing warning or protection capability. Likewise, the tactical advantages of near real-time signals intelligence (sigint) is being recognized with projects such as the S-3 Tactical Airborne Signals Exploitation System (TASES).

As envisioned, TASES will operate with the multi-mission carrier and provide passive early warning to the local tactical commander. The system will have a detection capability from HF to high J band and will possibly real time data link the information directly to the carrier. Since the TASES aircraft will be operating in a tactical environment, it will probably navigate and communicate using the standard Navy TACAN, UHF/ADF, and UHF comm frequencies. Also, there may be additional transmissions from a data link system.

The majority of these aircraft transmissions will probably be in the UHF range (particularly communication) and in a tactical environment specific frequencies may change often in the course of a normal mission. To prevent saturating an onboard UHF detection system, some isolation must be provided. The isolation can be handled by selectively blocking

appropriate frequencies, judicious location of antennas for minimum coupling or a combination of these techniques.

The frequency blocking method requires the passage of information from the transmitting system to the detection system that a frequency change is occurring. In the simple case, the pilot would tell the detection system operator that a frequency change would be made and the operator would manually block out the new frequency. This technique, while inexpensive, is fraught with potential human errors ranging from forgetfulness to misunderstanding. In total degeneration, the operator would simply block out the entire U.S. tactical UHF range and concentrate on other frequencies. Going to more complex frequency blocking systems, the human operators are taken out of the loop, being replaced by detectors and automatic switching systems with an attendant increase in cost and potential maintenance problems.

Clearly, if the systems could be decoupled at the antenna environment, the frequency blocking approach would be unnecessary. However, in the past there has been no reliable method of predicting antenna coupling on an aircraft. Instead, antenna systems have been usually designed based on past experience and educated guesses and then either tested on the actual aircraft or on brass models. Often this trial and error method has proved more costly than the alternative of using the complex blocking method.

Ideally, a computer simulation method can be found that will accurately predict the on aircraft performance and coupling of antennas.

B. BACKGROUND

1. Method of Moments

The performance of an aerial mounted on a conducting body such as an aircraft depends on the currents induced on the whole structure. At frequencies where dimensions of the body are comparable with wavelength, the approximate current distribution may be found using the "method of moments" (MM). This is a numerical technique for solving an integral equation, in this case the equation for the current distribution, by converting it to a matrix equation using a suitable segmentation scheme. Two segmentation methods have been used thus far, namely, the patch and the wire grid methods [Ref. 1].

In the patch method, the body is divided into a number of patches, each small in terms of wavelength. The wire grid method uses a wire grid to represent the body and is based on the principle that a wire mesh is equivalent to a conducting sheet provided the mesh spacing is small in terms of wavelength. The current on an individual segment, surface patch or wire segment, is assumed to be constant or to obey a simple algebraic or trigometric law. The matrix equation is formed by finding the reaction or mutual impedance between pairs of segments, and the excitation vector representing the source points. The matrix equation is solved to obtain the approximate current distribution. The radiation pattern may then readily be obtained by summing the contributions from individual segments.

Applications of the surface patch method to irregular bodies requires a surface representation with continuous curvature [Ref. 2] whereas straight wire segments are adequate to define the outline of the body, although more segments may be required. The surface patch method also leads to difficulties when applied to bodies with sharp discontinuities such as aircraft wings. Thus, wire grid modelling has been more extensively applied to aerial problems [Refs. 3, 4, 5]. Knepp [Ref. 2] has used the surface patch method to compute the radiation pattern of an aerial mounted on a CH-47 helicopter. There have been some attempts at a hybrid approach mixing the patch and wire methods.

Tanner [Ref. 6] has produced general computer methods for solution of antenna problems. These methods include direct integral approaches, and modelling structures with cylinders and wire mesh methods. His approach to the wire mesh problem allows a much larger grid spacing with an attendant decrease in matrix size and computer time.

In all cases except Tanner's, MM has been considered a low frequency technique for aircraft limited to frequencies in which the aircraft is of the order of one wavelength in size.

2. Geometrical Theory of Diffraction

Another successful approach to solving aircraft type problems is the Geometrical Theory of Diffraction (GTD). GTD has been considered a high frequency technique and is applicable to bodies that are arbitrarily large in an electrical

sense [Refs. 7, 8, 9]. The GTD solution is made up of two parts, namely, wedge diffraction and curved surface diffraction.

Using this approach, one applies a ray optics technique to determine the fields incident on the various scatterers. Diffracted fields are found, using the GTD solutions, as rays which are summed with geometrical optics terms to give a far field solution. Rays from any given scatterer will further diffract and reflect from nearby structures causing various "higher order" terms to appear. The various possible combinations of rays that interact between the scatterers can be traced out and determined, and typically include only the dominant terms. Thus at high frequencies, only the most basic structure features of the aircraft need to be modelled.

3. Hybrid Techniques

There has been effort recently to combine the MM and GTD methods. This has included approaching the problem by expanding the MM technique to include GTD methods [Ref. 9] and the reverse approach of extending GTD via MM by Burnside at Ohio State University.

Both of these hybrid techniques allow investigation of problems that were not solvable with MM or GTD alone. The results have just been published recently and appear encouraging.

A further discussion of all of these techniques will follow in the analysis section. Each has its capabilities

and limitations and will be examined in light of the UHF coupling problem.

C. STATEMENT OF THE PROBLEM

The remainder of this paper examines the various computer programs available to model the coupling of two UHF stub antennas on an aircraft. The UHF antennas are modelled as nine inch (.23 meter) whips with a bottom feed. It is recognized that actual UHF blade antennas are multi-element and driven differently (for broad band) but consultation with NADC (telephone conversation with Joe Miller) indicates that it is common to model the UHF antenna this way. Also, NADC indicated that a realistic termination impedance would be seventy ohms and the gain of standard UHF antennas is about 1.8 db over isotropic.

Three hundred megahertz is the only frequency examined.

II. METHOD OF ANALYSIS

A. DEFINITION AND THEORY OF COUPLING

In regard to antenna problems, coupling is defined as an indication of the quality and quantity of energy received at one antenna from another antenna. It is conveniently expressed in a coupling coefficient defined as

$$C = \frac{P_r}{P_t} \tag{1}$$

where P_r is the total received power and P_t is the total transmitted power. The coupling coefficient relates, for a given radiator and receptor, the power received to the power transmitted. The coupling coefficient is a function of the source, path and receptor parameters.

For an ideal case, conventional calculation techniques can be used to determine the far field coupling coefficient. Looking at coupling between a given set of antennas, the power density at any point in space due to the transmitting antenna can be expressed as

$$P_d = \frac{P_t \, G_t(\theta,\phi,\lambda)}{4\pi R^2} \tag{2}$$

where G_t describes the transmitting antenna gain as a function of frequency and spatial position. The effective capture area of the receiver antenna is

$$A_r = \frac{G_r(\theta,\phi,\lambda)\lambda^2}{4\pi} \tag{3}$$

where G_r describes the gain characteristics of the antenna. The total received power is

$$P_r = \frac{P_t G_t(\theta,\phi,\lambda) G_r(\theta,\phi,\lambda) \lambda^2}{(4\pi R)^2} \tag{4}$$

And the coupling coefficient is

$$C = \frac{P_r}{P_t} = \frac{G_t(\theta,\phi,\lambda(G_r(\theta,\phi,\lambda)\lambda^2}{(4\pi R)^2} \tag{5}$$

Note that the coupling coefficient is a function of the product of the two antenna gains.

Consider two short dipoles (length less than a quarter wavelength), parallel in space. For this case

$$G_t(\theta,\phi,\lambda) = G_r(\theta,\phi,\lambda) = 3/2 \sin^2 \theta \tag{6}$$

so that the coupling coefficient becomes

$$C = \frac{(3/2)^2(\sin\theta)^4\lambda^2}{(4\pi R)^2} \tag{7}$$

It is interesting to note that the NADC rule of thumb for blade antennas of 1.8 db gain is virtually identical to the 3/2 coefficient in equation (6)!

From Rockway [Ref. 10], the effective area of a monopole on a ground plane is

$$A_e = \frac{G_r \lambda^2}{16 \pi} \tag{8}$$

hus it can be seen that equation (7) also applies to a short monopole in a ground plane.

For a one-quarter wavelength monopole on a ground plane the gain is

$$G_r = 3.28 \left[\frac{\cos(\pi/2 \cos\theta)}{\sin\theta}\right]^2 \tag{9}$$

and the coupling coefficient becomes

$$C = \frac{(3.28)^2 \left[\frac{\cos(\pi/2 \cos\theta)}{\sin\theta}\right]^4 \lambda^2}{2^2 (4\pi R)^2} \qquad (10)$$

B. METHOD OF MOMENTS (AMP) GROUND PLANE ANALYSIS

MB Associates Information Systems Division of California has developed a comprehensive program using wire grid modelling known as AMP (Antenna Modelling Program) [Ref. 11] which was available for use at the Naval Postgraduate School. This program was developed under a government contract as a general aerial design tool.

The AMP program is based on a rigorous integral equation for the antenna current which is solved numerically using matrix manipulation techniques. A sinusoidal interpolation scheme is used to define the current distribution on individual wire segments. The current is made up of three terms. I_j the current on the j^{th} segment is given by

$$I_j(s) = A_j + B_j \sin k(s - s_j) + C_j \cos k(s - s_j) \qquad (11)$$

where s is the distance measured along the wire, for s in s_j defines the j^{th} segment and s_j is the midpoint of the j^{th} segment, $k = 2\pi/\lambda$, λ is the free space wavelength. The coefficients (A, B, and C) are obtained by enforcing the requirement that the extrapolated current from a given segment matches the midpoint current in two adjacent segments [Ref. 3]. The average midpoint current is used for multi-segment junctions. The integration for the sine and cosine terms in the impedance calculation have analytic solutions

but numeric integration is required for the constant current term. Kirchhoff's current law is enforced at all intersections.

The sinusoidal interpolation technique gives good results for wire aerials where segments of equal length can be used and where there are no multi-segment junctions because the current discontinuities are then very small. However, where there are junctions between several segments of different length there is a larger discontinuity. In modelling irregular bodies this must be kept in mind.

This approach is valid for any frequency and any structure size to wavelength ratio [Ref. 11]. However, it is recommended to keep segment lengths to less than one-tenth wavelength and grid spacings for solid surfaces to about the same size. Reference 11 leaves open the prospect, however, that somewhat longer segments may be acceptable on long wires with no abrupt changes. It should be remembered that the size of the segments determines the resolution in solving for the current on the model since the current is computed at the center point of each segment.

With the above restrictions in mind, the AMP program has most commonly been applied to wire antennas and problems in the HF and UHF bands.

AMP offers many options in modelling the antenna environment including placing other wire structures nearby, using series or parallel R-L-C circuits, terminal networks and transmission lines.

As a check on the theoretical results of coupling coefficients in the previous section, a series of AMP runs were made using .23 meter monopoles of .0001 meter diameter on a ground plane. The antennas were split into 15 equal segments. The transmitting antenna was fed at the base with a voltage source and the receiving antenna was terminated at the base with a 70 ohm resistance. The antennas were spaced at various distances and the transmitted and received powers were calculated.

The AMP program gives a direct output of radiated power. Received power was calculated from the output of the current in the 70 ohm element from $P_r = i^2 R$ (R is resistance, i.e., 70 ohm, here). The coupling coefficients were calculated with equation (1).

See Table I for a comparison of these results. The comparison for ground planes show reasonable agreement with theoretical results. The lower coupling of the AMP antennas is probably due to the less than optimum impedance match on the receiver antenna. The constant ratio of error in the AMP-divided-by-the-quarter-wave-theoretical-result column lends support to the hypothesis that the difference is consistant and due to the difference in the model. At the one meter point, the near field solution included in AMP can also be seen in the error ratio change.

The results for the ground plane analysis should be applicable to antenna arrays on large flat surfaces where the antennas are mounted at least 2 to 3 wavelengths from

an edge. The upper surface of a C-5A wing or its lower fuselage are examples of such cases.

TABLE I

Theoretical Coupling Coefficients
Compared to AMP Results

Distance Meters	Ceqn (7)* Short Monopole Ground Plane	Ceqn (10) /4 Monopole Ground Plane	AMP .23m Monopole Ground Plane	AMP/C (10)
1.0	-18.46	-17.67	-19.32	-1.65
2.7	-27.09	-26.29	-27.51	-1.22
5.0	-32.44	-31.65	-32.91	-1.26
8.0	-36.52	-35.73	-36.97	-1.24
10.0	-38.46	-37.67	-38.91	-1.24
12.2	-40.19	-39.39	-40.63	-1.24

*Coupling coefficients expressed in db.

An attempt was made to use AMP to calculate coupling over a plate. The 220 segment, one meter plate described in section II. E. was used with a source antenna at its center and a receive antenna at various locations on the plate. The source and receive antennas were the same .23 meter whips used in the ground plane analysis above. Comparative ground plane and theoretical results using equation (10) were calculated. The results are shown in Table II.

TABLE II

Coupling Coefficients over a Grid

Distance Meters	C* Eqn (10)	C AMP g.p.	C AMP grid	$C_{grid}/C_{g.p.}$
.25	-5.63	-9.54	-43.99 (on plate)	-34.35
.50	-11.65	-14.26	-50.47 (edge)	-36.21
.707	-14.66	-16.38	-44.42 (corner)	-28.04

*All coefficients in db.

It had been hoped that the AMP grid coupling could give an indication of the effects of a flat plate edge (as near the edge of a wing) on the coupling coefficient. The greatly lower values of coupling coefficient calculated by AMP indicates that the surface is probably not being modelled sufficiently accurately to give valid near field results. A finer grid is probably needed to improve the quantitative results. The grid coupling results show a difference of 28-36dB. The grid is not acting as a ground plane.

While the quantitative results for this trial were less than encouraging, the qualitative information is of more interest. The results from equation (10) were included to indicate how it breaks down calculating near field information. The effective aperature assumption for this equation makes it invalid at these close distances. The three positions of coupling calculation over the grid were at a point equidistant to an edge (.25m), on the middle of an edge (.50m), and on a corner (.707m). Using the "on plate" point (.25m) as a base, the edge coupling point had dropped 6.48dB as opposed to a change for that distance in the ground plane calculations of 4.72dB. This result, that coupling was decreased by moving the receive antenna near an edge, was expected. However, the corner data point shows increased vice a further decrease in coupling. Again, using the .25m point as a base, the corner coupling coefficient drops only .43dB whereas the same distance change over a ground plane causes a drop of 6.84dB.

Again it is emphasized that no firm faith can be placed in the accuracy of these results in predicting a real world situation. The grid spacing is obviously not correct to properly model a solid plate in the near field. The corner increase in coupling could be due to a corner diffraction effect or simply to a built-in anomoly in the model.

Clearly, more runs need to be studied with varied geometries to test the above results. As a first step, diagonal cross elements in the vicinity of the receive antenna or a finer grid should be tried. However, it is to be considered that these runs with 250 elements averaged 29 minutes of computer time on the NPS IBM 360/67. Due to this time problem, further studies were not attempted in this area.

C. AMP LIMITATIONS

The greatest limitation on AMP comes from the restriction to model wire segments in lengths of one-tenth wavelength or less and to model surfaces with a grid of the same order to obtain reasonably accurate results. Thus, surfaces of one square wavelength require at least 200 segments, a one wavelength cube at least 1200 segments, etc. As can be seen, the problem gets out of hand quickly. The AMP program has been issued in three versions allowing either 250, 500, or 1000 segments depending on the accuracy of the machine on which it is to be used. There is a fundamental limitation on the size of matrices which modern computers can invert without excessive loss of accuracy. So, as a rule of thumb, AMP should not be applied to complex structures of greater than

one or two wavelengths in size. Obviously, applying this restriction to the 300 megahertz frequency of this study limits application to shapes on the order of one to two meters -- far from the desire of modelling an aircraft.

Figure 1 shows some typical run times of AMP programs for various numbers of segments. The NPGS computer terminal time accounting routine is only accurate to plus or minus about ten percent depending on other jobs in the system.

Several schemes were investigated to try to increase the size that AMP could handle. Using coordinate reflection techniques to maintain matrix symmetry only yielded an increase of a factor of four for a full reflection in two axes. An interesting technique was found to eliminate unwanted structure caused by the reflection. The unwanted portions can be connected together two at a time with net work (NT) cards that have zero values entered and the segments disappear as far as affecting the solution.

Tests were run with larger spacings and segment size to get a handle on the one-tenth wavelength restriction. A two wavelength square was modelled with wires around the outer edge, across the diagonals and connecting the midpoints of opposite sides. The wires were split into segments of one-tenth wavelength. The feed was placed one-quarter wavelength above the center of the "plate." The resulting radiation pattern indicated that the plate was almost totally transparent! Various other tests were run and all confirmed the one-tenth wavelength limitation for this plate problem.

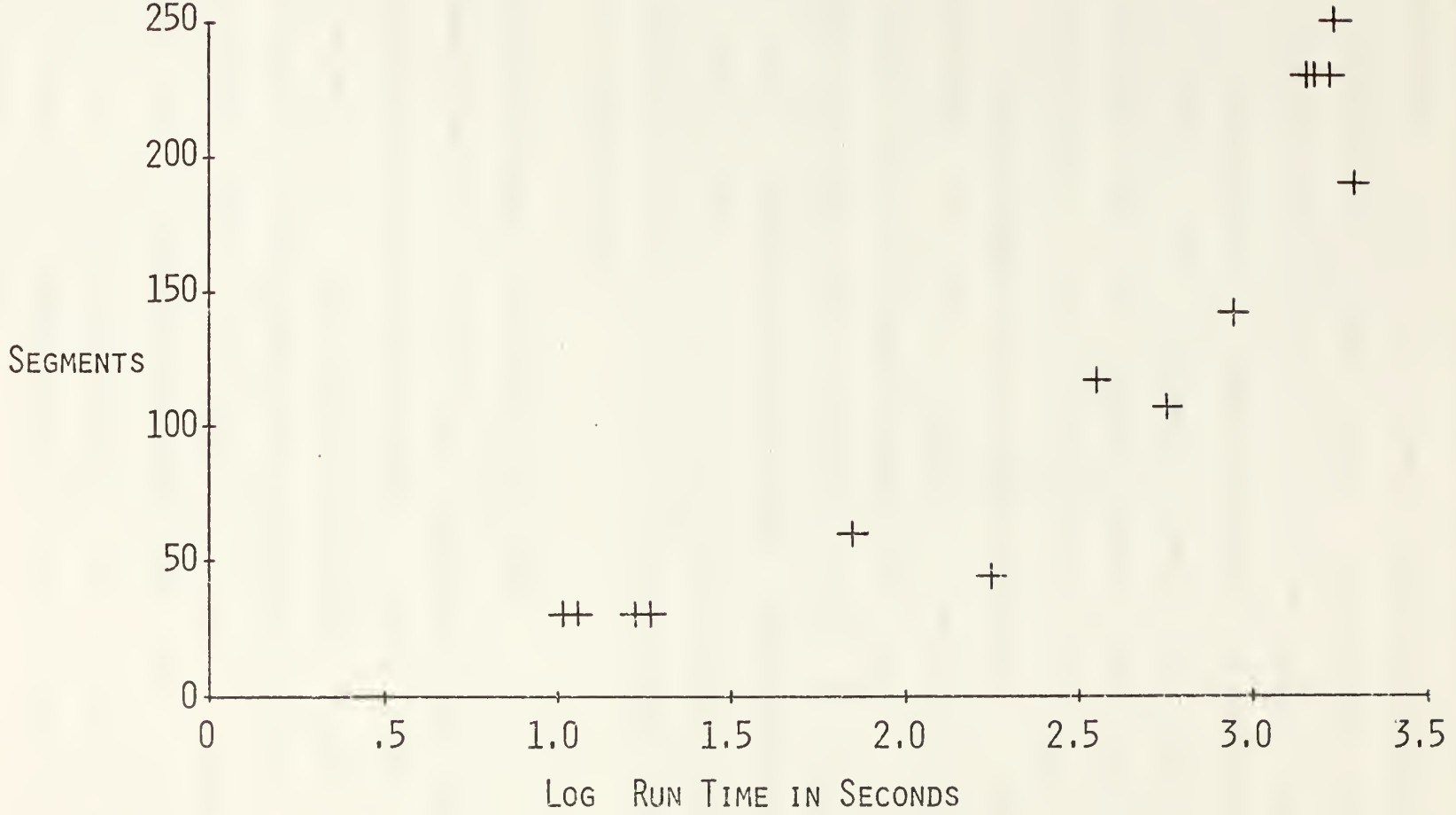

FIG.1. AMP RUN TIME

One notable exception to the transparency problem of coarse grid models was a wing model that shows a fair degree of correlation to results of a similar wing from the BENT program explained in the next section. The results surprised this investigator and are presented to show one of the pitfalls lurking in this approach. Some structures can be modelled in a very crude manner and "reasonable" results achieved, whereas other structures even with virtually exact modelling will provide erroneous data as with the Bell 47G-4A helicopter in [Ref. 4]. The segmented wing is shown in Figure 2. The results for AMP and BENT are shown in Figure 3. The field cut is in the Y-Z plane with zero degrees along the Z axis.

Attempts were also made to model the edge of a wing using the cliff or wire screen options in AMP. None of these approaches proved viable. The cliff problem only affected far field radiation pattern results and the wire screen had to be placed on a ground plane.

D. GEOMETRICAL THEORY OF DIFFRACTION (GTD)

W. Dennis Burnside of Ohio State University has done extensive work using the GTD technique to study radiation patterns on aircraft. This work has included a series of Navy contracts which have resulted in two computer programs.

The original effort was to produce a computer program that would nearly exactly model an aircraft shape with cylinders, cones, portions of spheres and plates. Also, attempts have been made to model the fuselage with a convex surface of revolution [Refs. 7 and 8].

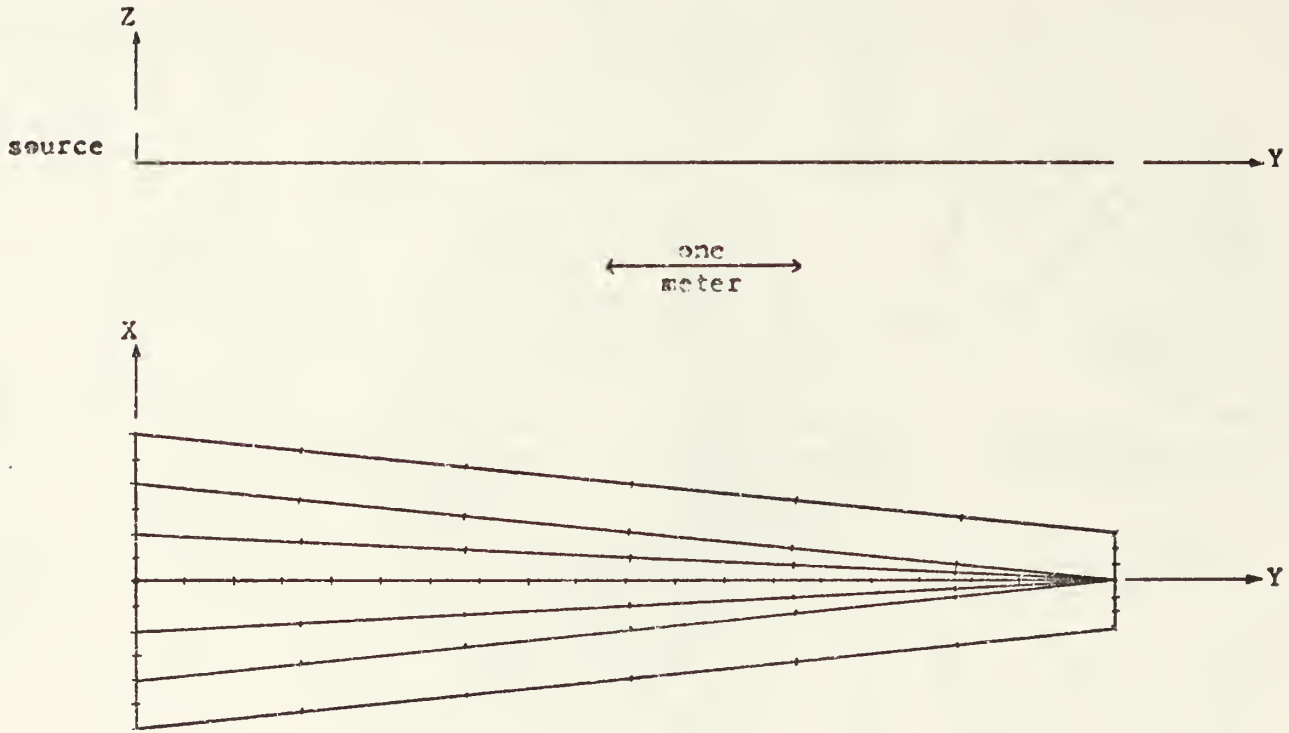

FIG.2. GROSS AMP MODEL OF WING IN BENT SAMPLE
(FEED AT 4.72 INCHES) RIGHT HALF ONLY SHOWN

WING

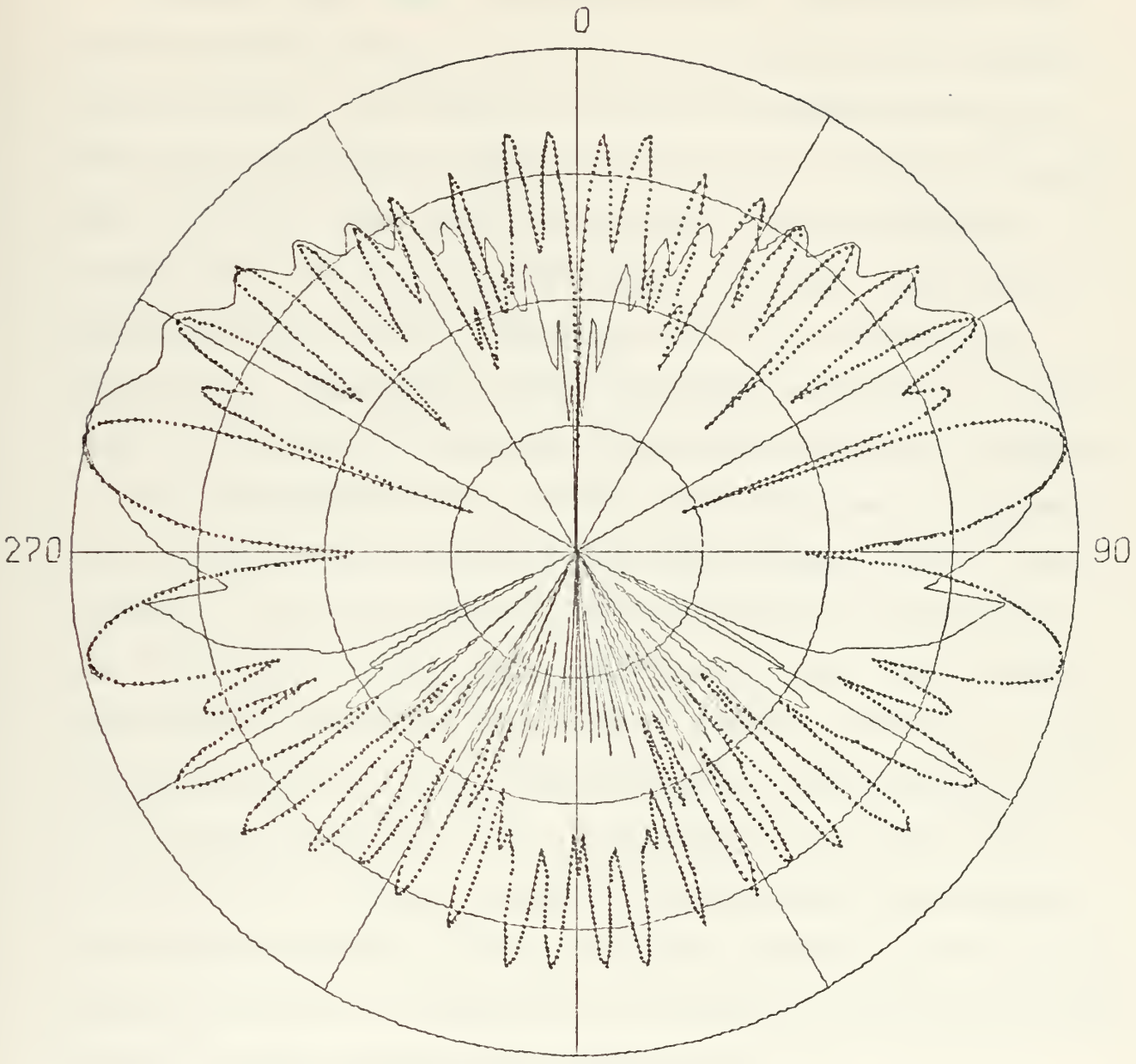

E-PHI DB PLOT 40 DB SCALE
NO. OF CORNERS OF PLATE= 6
ROTATION ANGLE OF PLATE= 180.000
FREQUENCY= 0.300
ANTENNA TYPE= 4.72" FEED
THETA ROTATION ANGLE OF DIPOLE= 90.000
PHI ROTATION ANGLE OF DIPOLE= 0.000
PATTERN NO. FLAT
BENT IS SOLID LINE, AMP BROKEN

FIG.3. BENT/AMP WING COMPARISON

Results with shapes other than plates and elliptic cross section infinite length cylinders have been less than encouraging thus far. Two computer programs are now held by the Naval Air Development Center, Warminster, Pa. These are named ROLL and BENT. ROLL models an aircraft with an elliptic cylinder for the fuselage and plates for wings. BENT is a simplification of ROLL, examining only flat or bent plate situations. Each program had a potential application in the coupling problem and therefore copies were obtained from NADC.

It is appropriate to note here that there was no documentation done on these programs save some comment cards in the program. Also, the programs had been written at Ohio State for an IBM 360 and then modified for use on the NADC CDC6600. Also, modifications had been made at NADC for different output. The NPS computer is an IBM 360/67 but the tape from NADC was in a different character set, had incompatible typed output and pen plotter output. Without documentation, the cleaning up of these programs for use on the NPS computer proved tedious and time consuming. Appendix A is included to shed some light on use of these programs for future users.

As indicated in the introduction, these programs use a ray optics technique to solve for a field. The primary components of the energy at a point in a field are direct, reflected and diffracted energy. The approach in obtaining the field for a structure is to calculate all the components (direct, reflected and diffracted) from each surface at one point in space and sum them.

The frequency range of application of this method is not clear. Input is given in gigahertz. Reference [7] calls it a high frequency technique and [Ref. 8] includes information on a light pen adaptation of the program with selectable frequencies from one to ten gigahertz. Discussion with various individuals indicated that the GTD approach was limited to microwave frequencies.

It was originally hoped that the programs could be modified to give near field and near structure field strengths. This has not been accomplished to date. One initial problem in this area is that the source and various scattering centers be separated by at least a wavelength. This restriction ties in with the lowest usable frequency discussion in the previous paragraph.

The sample programs in Appendix A give some indication of the input/output combinations available.

It is interesting to compare the plot outputs of Appendix A. The ROLL solution includes the effects of the infinite cylinder whereas BENT does not. Past forty-five degrees from vertical, the patterns are virtually identical. The sharp step at about 100 and 260 degrees is probably caused by the program switching calculating schemes from direct and reflected to diffracted. These steps seem to occur more often when there are shallow grazing angles from source to edge. This indicates that the diffraction coefficients used are not precise at shallow angles because they include only first order effects. Generally, the true field pattern appears to be a faired curve through the jump.

E. BENT/AMP COMPARISONS

As discussed earlier, BENT is supposedly restricted from use at other than microwave frequencies and with a feed closer than one wavelength. This limitation is due to the inaccuracy of the diffraction coefficients at low angles. However, these restrictions were discovered after successfully running a two meter flat plate with a feed at .1 meter from the center at 300 megahertz. It seemed to give results that were reasonable.

As discussed in section II. C. above, it was shown that for reasonable results with AMP, the surface must be modelled with a grid that has segments and holes no larger than .1 wavelength. This means that there must be about 200 segments plus final edge segments per square wavelength of surface. Also, as the segments in AMP increased over 200 the run time became 20 to 30 minutes and two-day turnarounds became normal at the NPS computer facility. Thus at 300 MHZ the maximum realistic surface was one square meter.

It was decided to run a comparative study of the BENT and AMP programs to get a better grasp on the above limitations. A one-square meter plate was modelled with both BENT and AMP. The feed was placed at .08, .5, and 1.0 meter positions above the center of the plate as in Figure 4. In Figures 5 through 8 the results of this comparison are shown.

Reasonably high confidence is placed in the AMP results due to the fineness of the grid and the past history of AMP data. The feed in AMP was a .1 meter whip divided into ten segments and fed from the lower segment. It was positioned

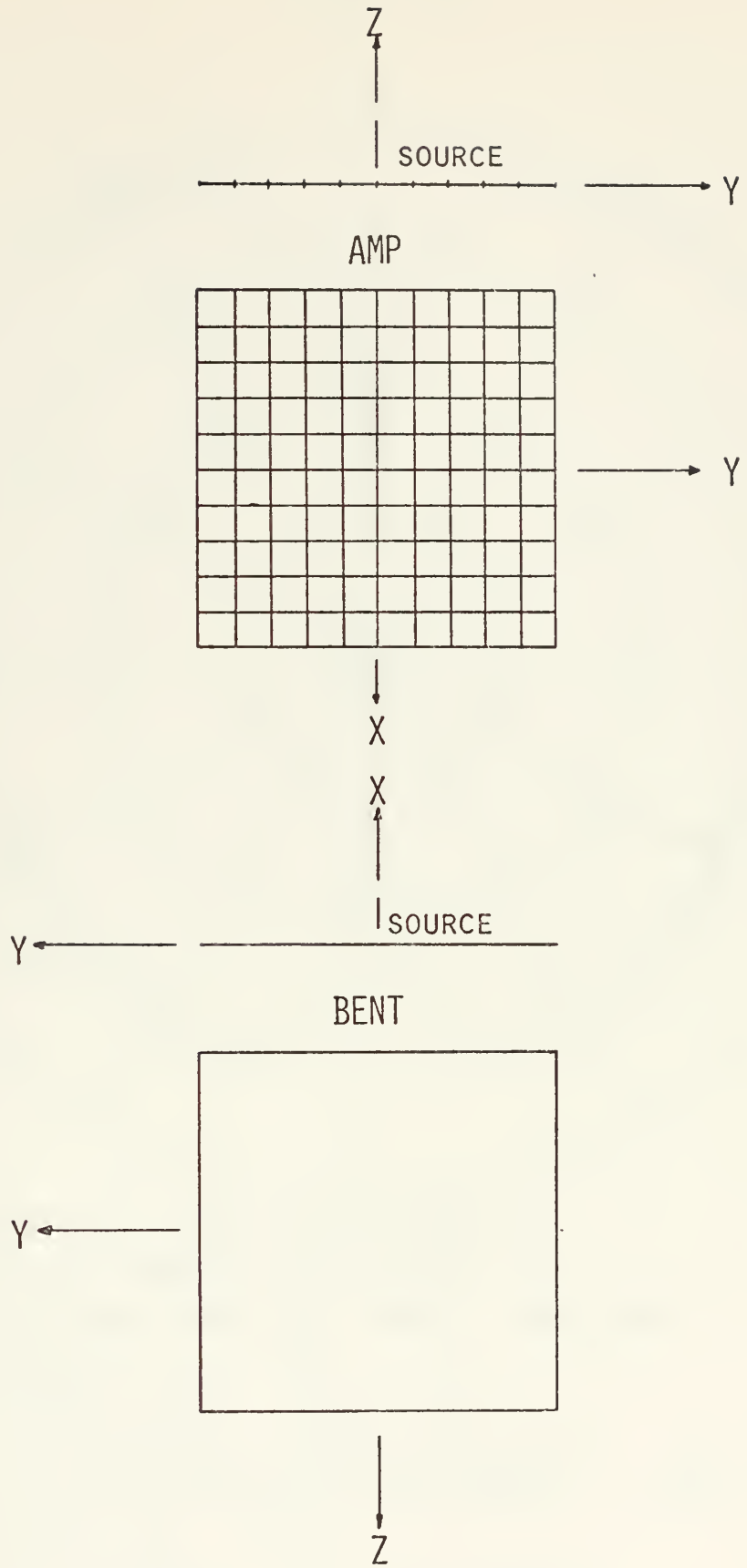

FIG.4. GEOMETRY OF FLAT PLATE

PLATE

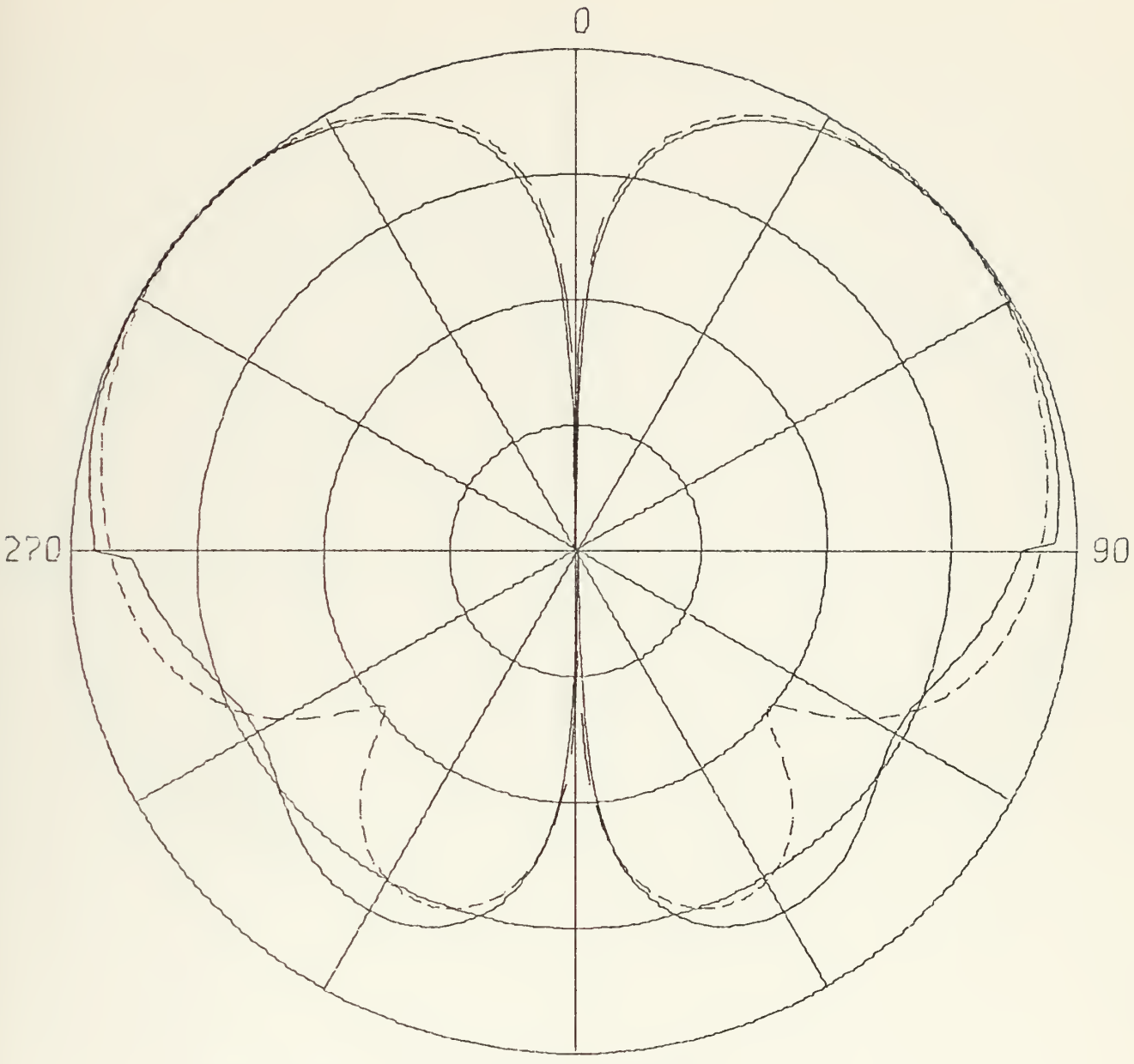

E-PHI DB PLOT 40 DB SCALE
NO. OF CORNERS OF PLATE= 4
ROTATION ANGLE OF PLATE= 180.000
FREQUENCY= 0.300
ANTENNA TYPE= 0.08M FEED
THETA ROTATION ANGLE OF DIPOLE= 90.000
PHI ROTATION ANGLE OF DIPOLE= 0.000
PATTERN NO. PLATE
BENT IS SOLID LINE, AMP BROKEN

FIG.5. FLAT PLATE BENT/AMP COMPARISON, .08M FEED

PLATE

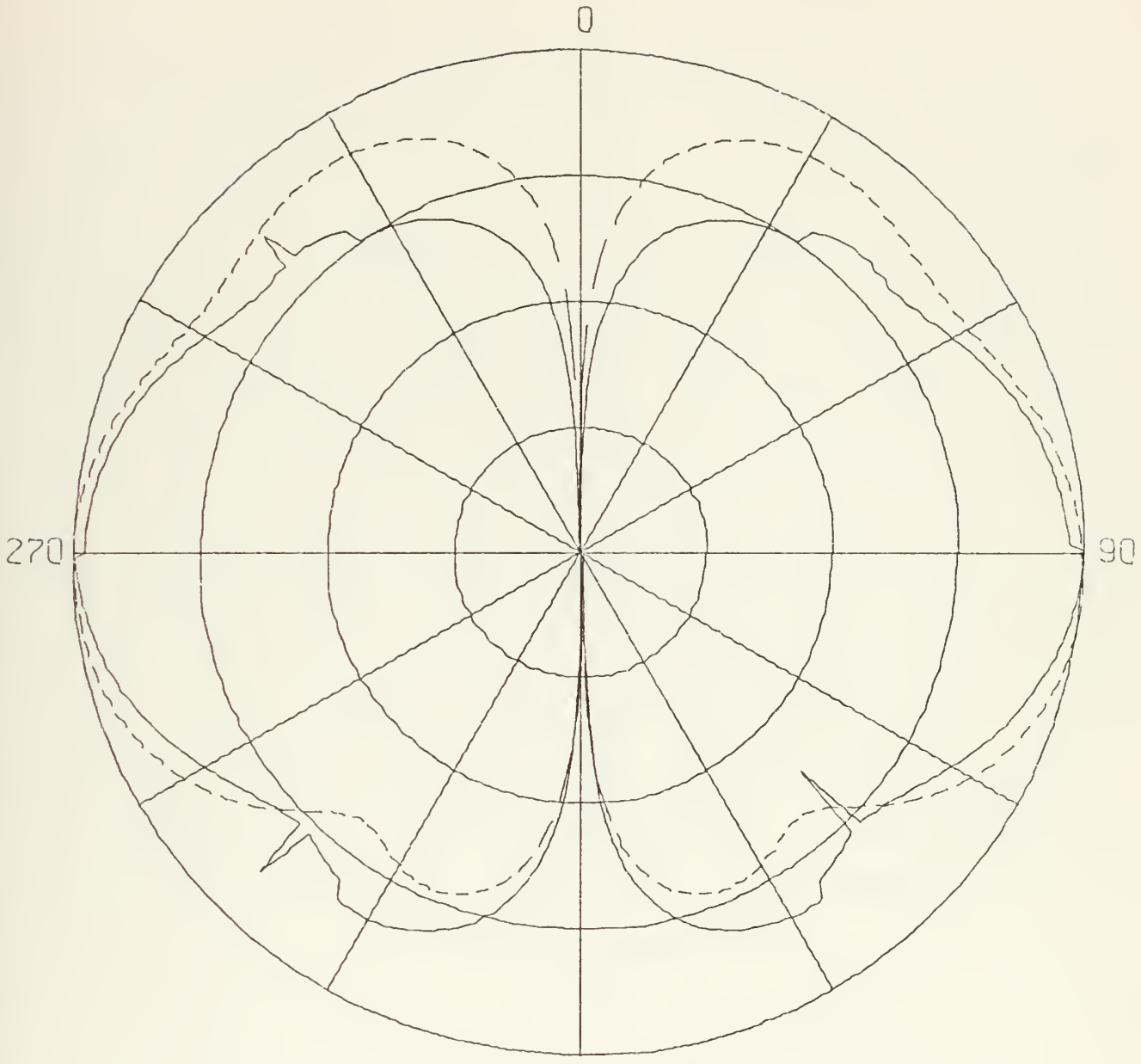

E-PHI DB PLOT 40 DB SCALE
NO. OF CORNERS OF PLATE= 4
ROTATION ANGLE OF PLATE= 180.000
FREQUENCY= 0.300
ANTENNA TYPE= .5M FEED
THETA ROTATION ANGLE OF DIPOLE= 90.000
PHI ROTATION ANGLE OF DIPOLE= 0.000
PATTERN NO. PLATE
BENT IS SOLID LINE, AMP BROKEN

FIG.6. FLAT PLATE BENT/AMP COMPARISON, .5M FEED

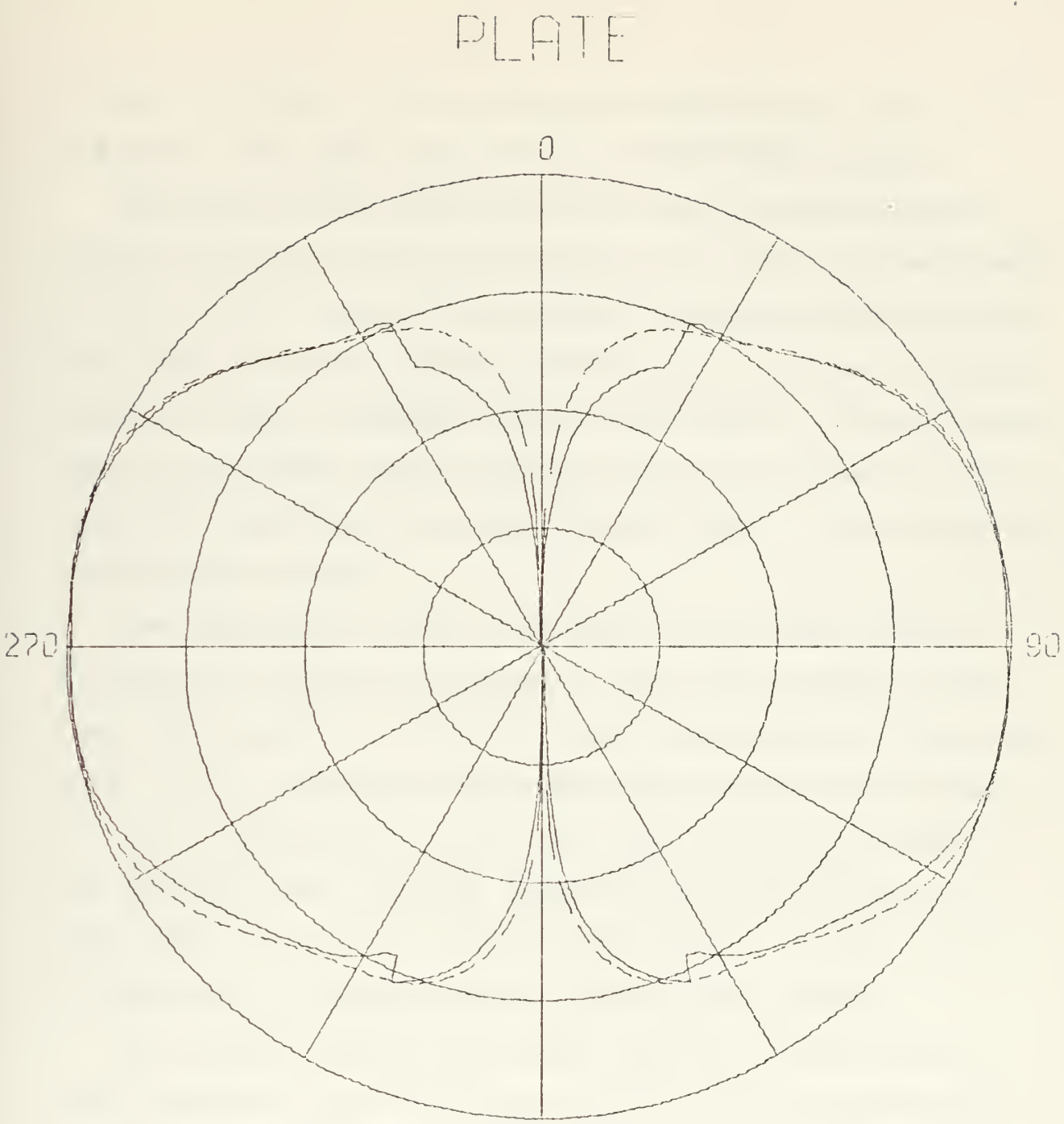

E-PHI DB PLOT 40 DB SCALE
NO. OF CORNERS OF PLATE= 4
ROTATION ANGLE OF PLATE= 180.000
FREQUENCY= 0.300
ANTENNA TYPE= 1M FEED
THETA ROTATION ANGLE OF DIPOLE= 90.000
PHI ROTATION ANGLE OF DIPOLE= 0.000
PATTERN NO. PLATE
BENT IS SOLID LINE, AMP BROKEN

FIG.7. FLAT PLATE BENT/AMP COMPARISON, 1.0M FEED

so that the point .03 meter from the bottom was at .08, .5 or 1.0 meter. The BENT source was an infinitesimal dipole.

The jumps in the BENT solutions usually occur when the program shifts methods of calculating the field. A good example of this is the step at 153.5 and 206.5 degrees on the .5 meter feed plot. Geometry of the problem shows that this is exactly where the region shadowed from the feed begins. Usually these bumps in the BENT solution can be just faired through. It is important, however, to be sure that the bump is from extraneous causes and not real.

The comparative results show that in this case the two methods are in general agreement. With the exception of the lower lobe nuances at .08 m feed and the magnitude of the upper lobes at .5 m feed, the two methods show surprising agreement.

It is interesting to note also that the average computer run time for BENT including compiling was less than two minutes (about 50 seconds compile time) and the average run time of AMP which is precompiled was twenty-seven minutes.

The results indicate that BENT will give usable data at UHF frequencies and at locations within a half wavelength of the surface. For small, square plates, apparently BENT may be applied with feeds essentially on the surface (.1 wavelength).

F. TCI RESULTS

Robert Tanner of Technology for Communications International was kind enough to calculate the one-meter plate problems of section II. E., using the TCI wire grid solving computer program.

His solutions are presented over the BENT/AMP solutions in Figures 8 through 10.

Tanner expressed great confidence in these results due to past experience with the TCI program.

The exact formulation of the TCI program is confidential within TCI but it is known that a wire grid technique is used. However, the grid spacing can be much larger than .1 wavelength. This is accomplished by recognizing that if a wire square is used to model a square patch of surface that the wire 'loop' will have more inductance and less capacitance than the plate. The TCI program takes this effect into account whereas AMP does not. Run times on the TCI CDC6600 computer were about 5 seconds.

G. HYBRID TECHNIQUES

Reference 9 shows one method of combining MM and GTD to expand these methods to problems, including a monopole next to a conducting edge and a monopole on a plate. The approach was to start with a MM formulation and modify the impedance matrix based on GTD considerations. The results show that the input impedance and reactance of a monopole near a conducting edge of 90 degrees (cliff) begin to oscillate above and below the input values on an infinite ground plane when the monopole is within about three wavelengths of the edge. The oscillations become most pronounced inside one wavelength and the approach generally broke down inside .2 wavelengths. Similar results were achieved for a monopole over an octagon, square and circular plate. The octagon results are better than the square since vertex diffraction is neglected.

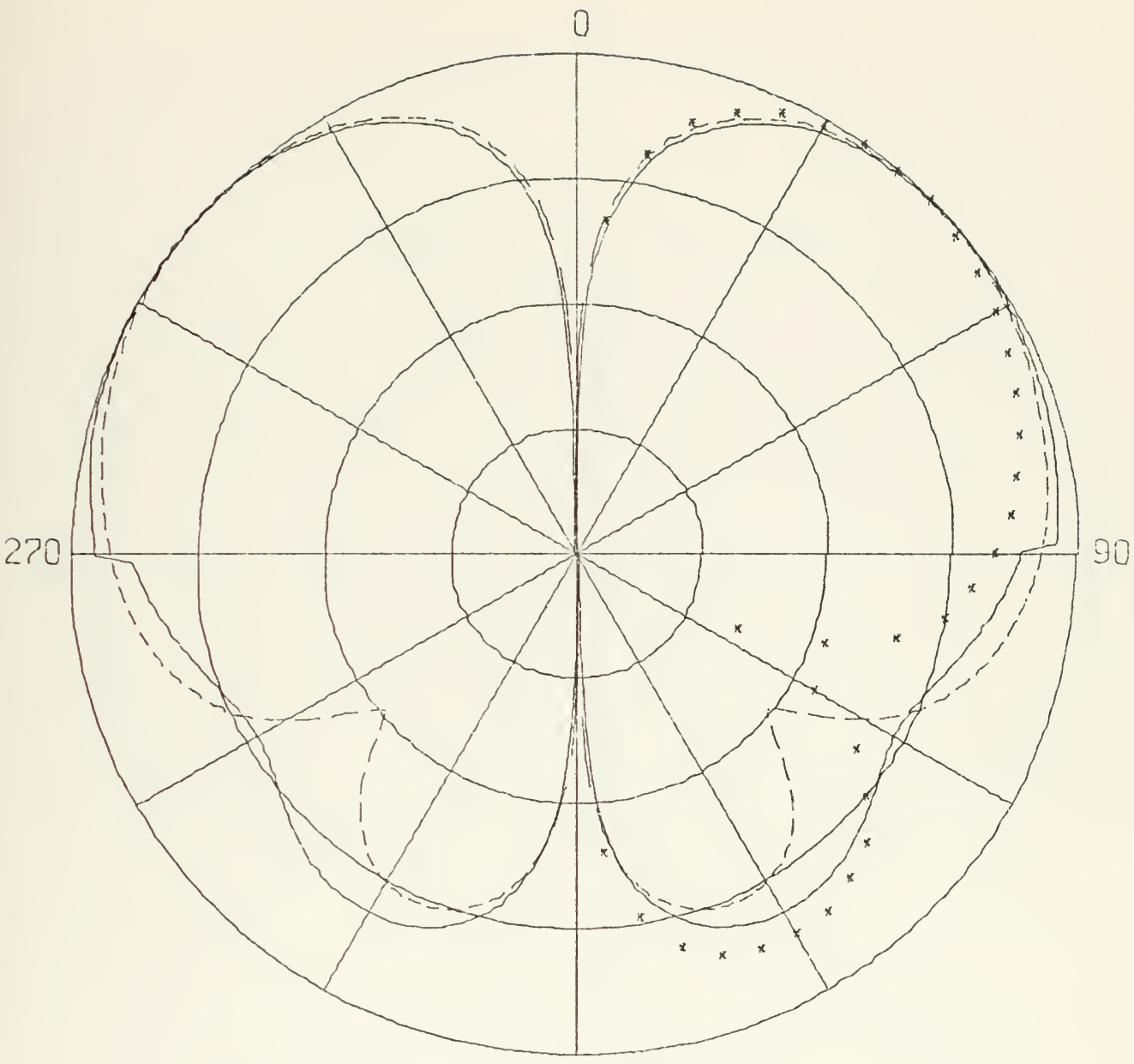

E-PHI DB PLOT 40 DB SCALE
NO. OF CORNERS OF PLATE= 4
ROTATION ANGLE OF PLATE= 180.000
FREQUENCY= 0.300
ANTENNA TYPE= 0.08M FEED
THETA ROTATION ANGLE OF DIPOLE= 90.000
PHI ROTATION ANGLE OF DIPOLE= 0.000
PATTERN NO. PLATE
BENT IS SOLID LINE, AMP BROKEN, TCI ASTERICK

FIG.8. BENT/AMP PLATE WITH TCI RESULTS, .08M FEED

PLATE

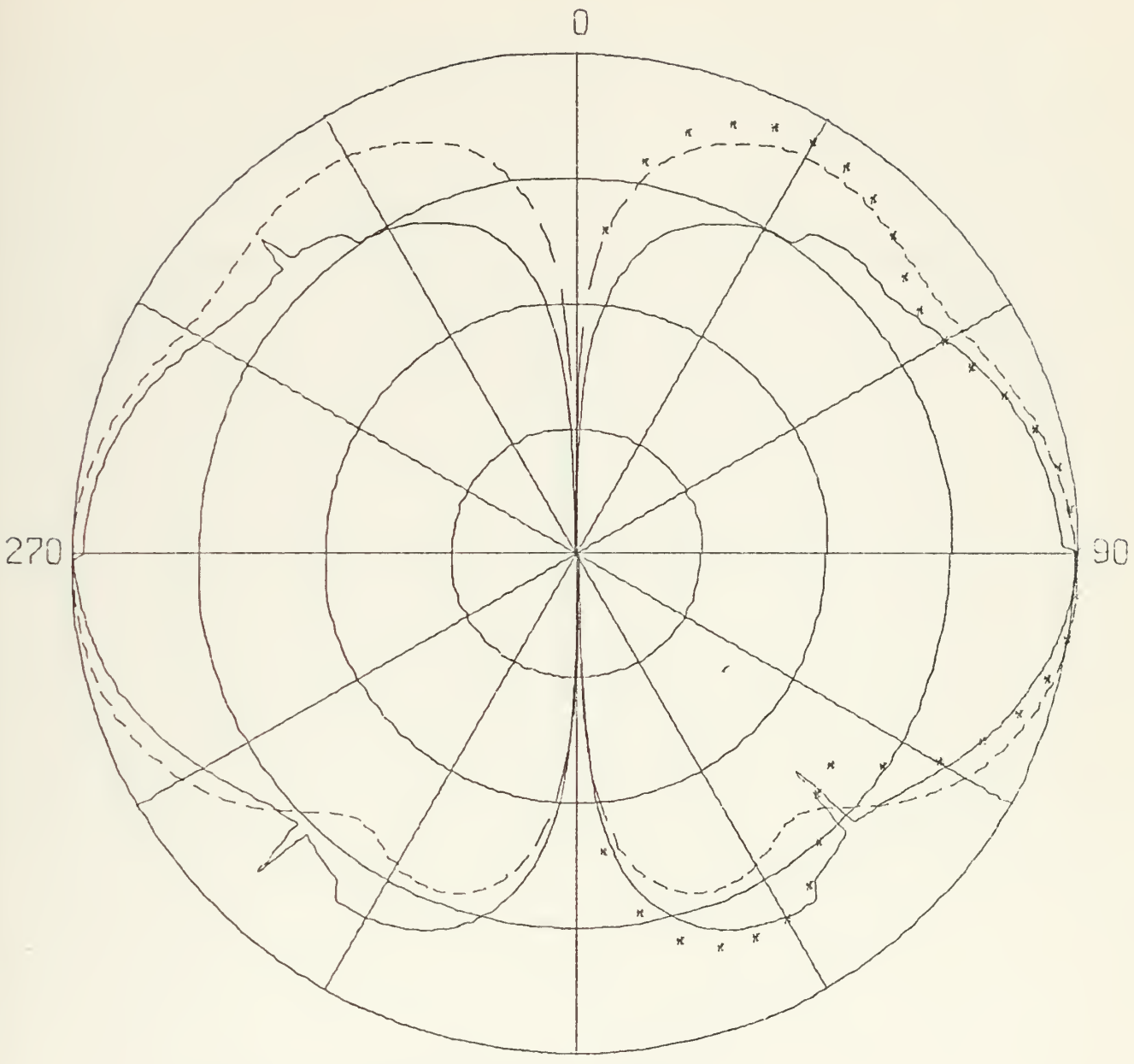

E-PHI DB PLOT 40 DB SCALE
NO. OF CORNERS OF PLATE= 4
ROTATION ANGLE OF PLATE= 180.000
FREQUENCY= 0.300
ANTENNA TYPE= .5M FEED
THETA ROTATION ANGLE OF DIPOLE= 90.000
PHI ROTATION ANGLE OF DIPOLE= 0.000
PATTERN NO. PLATE
BENT IS SOLID LINE, AMP BROKEN, TCI ASTERICK

FIG.9. BENT/AMP PLATE WITH TCI RESULTS, .5M FEED

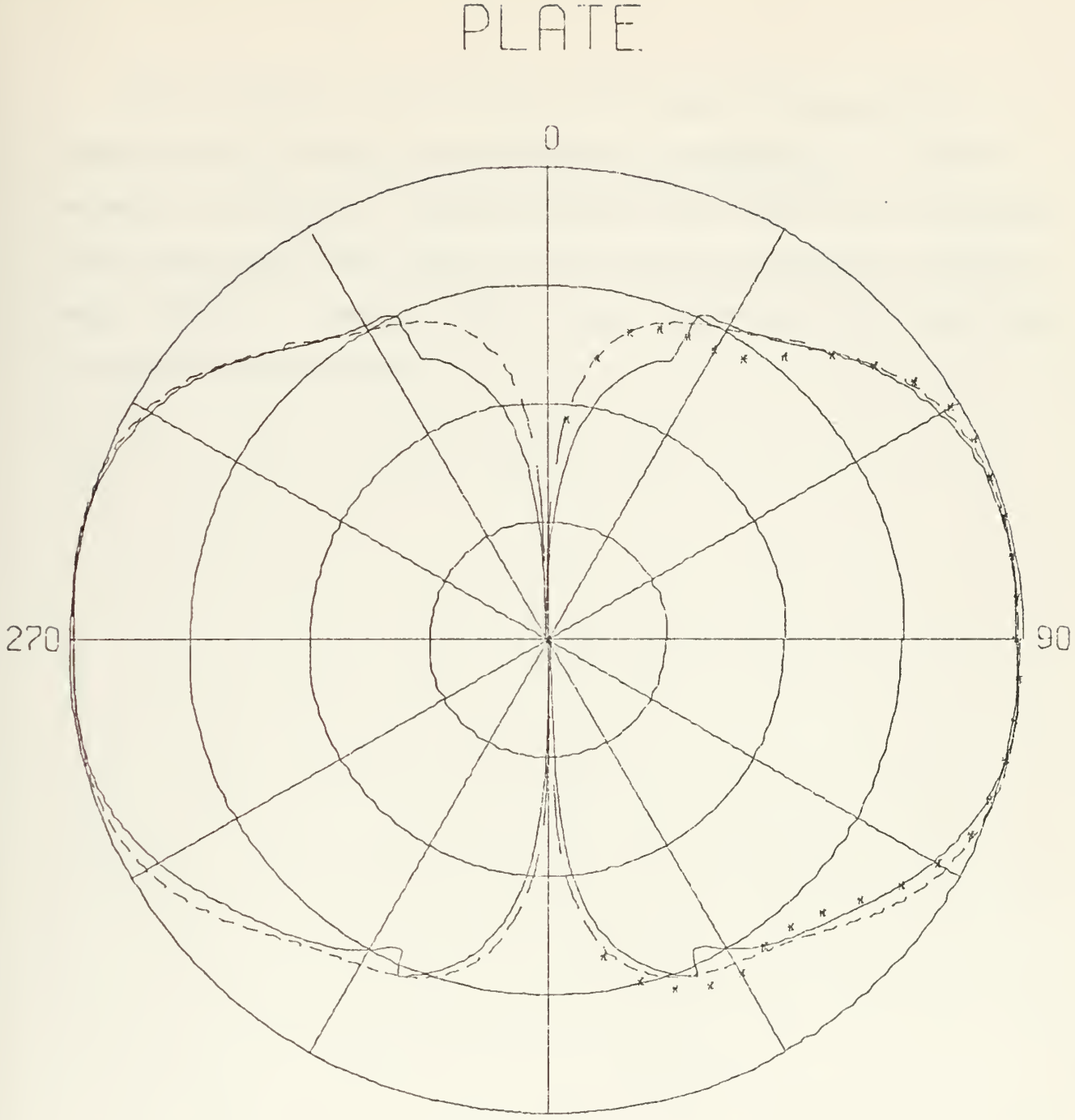

FIG.10. BENT/AMP PLATE WITH TCI RESULTS, 1.0M FEED

It was hoped to obtain far field data on this work to compare with the plate calculations in section II. E. and to attempt to calculate coupling coefficients with this technique. The conducting wedge and plate approaches seem ideal to model wing surfaces. However, due to time limitations this work has not been accomplished.

III. CONCLUSIONS AND RECOMMENDATIONS

The solution of antenna performance near complex conducting structures is still a problem. Computer techniques using moment methods, geometrical theory of diffraction and modifications and combinations thereof are useful for certain specific and generally simple problems, but no universal solution method is now available.

The MM technique is too cumbersome for application to structures much larger than one wavelength and the OSU GTD programs cannot be applied to the coupling problem since there are no near-field data (field within the size of the structure).

The data obtained from ground plane analysis using AMP indicates 1.24 db less coupling for real world UHF antennas than theory predicts. These results may be helpful in designing antenna arrays on large flat surfaces. However, these results have not been substantiated with actual measurements so they may still be optimistic or pessimistic.

The most promising method for solution of coupling problems appears to be a hybrid approach using GTD to modify the impedance matrix in an MM formulation. TCI's "modified" surface approach modifies the matrix in a similar manner. This method readily gives the current in the various segments and allows easy calculation of the coupling coefficients.

However, even with the most recently published hybrid methods, the solution of edge fields has yet to be addressed.

Also, more exact diffraction coefficients need to be developed to allow closer placement of sources and diffraction surfaces. The included results for a square plate show that in some cases, however, satisfactory results may be achieved with present coefficients. As the various methods become more refined, higher order terms that have so far been neglected will have to be considered, such as double diffraction and sharp angle corner diffraction.

APPENDIX - OSU GTD PROGRAMS "ROLL" AND "BENT"

I. ROLL PROGRAM

A. GENERAL

The OSU ROLL program combines an infinite cylinder of elliptic cross section with "wings" which may be bent once. The fields are calculated from contributions due to direct source energy, reflected energy and diffracted energy. The program calculates the fields from one wing, then adds on the fields from succeeding wings.

B. COMMENTS ON INPUT DATA

See Table A-I for a listing of input data and Figure A-1 for the coordinate system used.

It was found that THC and PHC cards had to be entered at some value other than zero, at least with the geometry of the sample problem. If entered as zero, the program would fail in subroutine SGTD on card 011450 in calculating TAN (AS). AS was 90 degrees. At this point SGTD was branched from FUSLAG which was branched from REFFD which was called from MAIN. Note that wing geometry must not penetrate fuselage. It is important that geometries closely coincide. They should be checked on a calculator. The NPGS computer is an IBM 360.

C. OUTPUT

The version of the program received at NPS had various minor output incompatabilities. Notably, all quotations

were double and had to be changed to single. Also, some formating of data was awkward, such as titles following immediately below data and then a page skipped prior to actual data listing. The POLPLT subroutine had to be rewritten to make it compatable with the NPS plot subroutine package. Fortunately, the ROLL authors and NPS both generally followed Calcomp's recommendations in plot subroutines.

The POLPLT subroutine plots either magnitude power or db polar plots. The plots are scaled to fit all data into the plot size indicated by RADC. In the main part of the program, E-theta and E-phi values are searched for the maximum. This is then called EMX. Within the POLPLT subroutine, RADC is called RP and E-theta or E-phi, as appropriate, is called ET (which is complex). An intermediate term is formed, ETM, which is the complex absolute value of ET divided by EMX. The radius of the point on the polar plot RD is found as follows:

For Field Plot:

```
RD = RP x ETM
```

For Power Plot:

```
RD = RP x ETM x ETM
```

For db Plot:

```
RD = 2D x ALOG10 (ETM)
IF (RD.LT. - 40) RD = -40
RD = RP x (RD + 40)/40
```

The logical LWRT (card 3) controls printing of intermediate values of the E-theta and E-phi field. Thus, for one wing, this is 722 lines of output -- for two wings, 1444, etc. The final listings of the field are not affected by LWRT.

Card 5 allows skewing of the field pattern axis. Note that ITHI, ITHF, etc., apply in this "new" coordinate rotation.

D. GEOMETRY

If the wings are located below the centerline of the fuselage, a tangent fillet from the widest point in the fuselage is dropped down to the wing.

The program "blows up" if the wings are placed on top of the fuselage with the source also on top, according to NADC.

E. SAMPLE DATA DECK

The data deck in Figure A-2 is for a mid-wing model with the fuselage 72 inches in diameter. The overall wing span is twenty meters with a three-meter root and even tapering to a one-meter tip. The wing is flat.

The source is the monopole and is located exactly over the center of the wing on the top of the fuselage. The monopole is oriented perpendicular to the plane of the wings. See Figure A-3 for a sketch of the sample problem. The field plot data is taken in the X-Y plane with the zero degree position corresponding to the positive X axis.

The polar plot output is shown in Figure A-4.

TABLE A-I

Input Format for ROLL

Card Number	Column Number	Description	Format
1	1-10 11-20 21-30	MP = Number of wings MX = Number of edges per wing FRQG = Frequency in gigahertz	2I10, F10.5
2	1-10 11-20 21-30 31-40 41-50 51-60	AF = One-half overall X-direction of fuselage BF = One-half overall Y-direction of fuselage PHSO = Angular position of source, in degrees, zero equals top of fuselage ZS = Z-coordinate of source JANT = Type of antenna (infinitesimal element) slot = 1 radial monopole = 2 BETA = Angle slot makes with Z-axis Note: Distances entered in inches	4F10.5 I10, F10.5
3	1-5 6-10 11-15	LWRT = Additional write-out desired (true or false) LPLT = Pattern plotted by pen plotter (true or false) LFLAT = Is flat plate considered (true or false)	3L5
4	 1-5 5-10 11-15 16-20	THETA and PHI are radiation angles ITHI = Initial value of THETA in degrees ITHF = Final value of THETA in degrees ITHS = Incremental step in THETA in degrees IPHS = Incremental step in PHI in degrees Note: If ITHI does not equal ITHF then cards after card 5 must be reentered for each step in THETA. Also, as the program is set up, IPHS = 1 always	4I5

TABLE A-1 (cont'd)

Card Number	Column Number	Description	Format
5	1-10 11-20	THC = THETA rotation angle of the axis of pattern rotation PHC = PHI rotation angle of the pattern rotation Note: Angles in degrees. ITHI and ITHF are values in this rotated coordinate system	2F10.5,
6	1-10 11-20 21-30	MC1 = Number of first corner at bend MC2 = Number of second corner at bend RTH = Angle of bent between surfaces Note: If wing is defined flat (LFLAT=T), then MC1=MC2=MX and RTH=180	2I10 F10.5
7 to 6+MX	1-10 11-20 21-30	X coordinate of a corner of the wing Y coordinate Z coordinate Note: Positions entered in inches. Points must be ordered counter clockwise, first point on fuselage. At no point may the wing plane enter the fuselage.	3F10.5,
7+MX	 1-10 11-12	Only used if LPLT = T RADC = Radius of polar plot on pen plotter IPLT = Field Plot = 1 Power Plot = 2 DB Plot = 3 If more than one wing is called for (MP greater than 1), then repeat cards 6 and 7 to MX with the appropriate coordinates for new wing. If ITHI does not equal ITHF, then all cards from first card 6 on must be repeated for each step in THETA.	 F10.5, I2

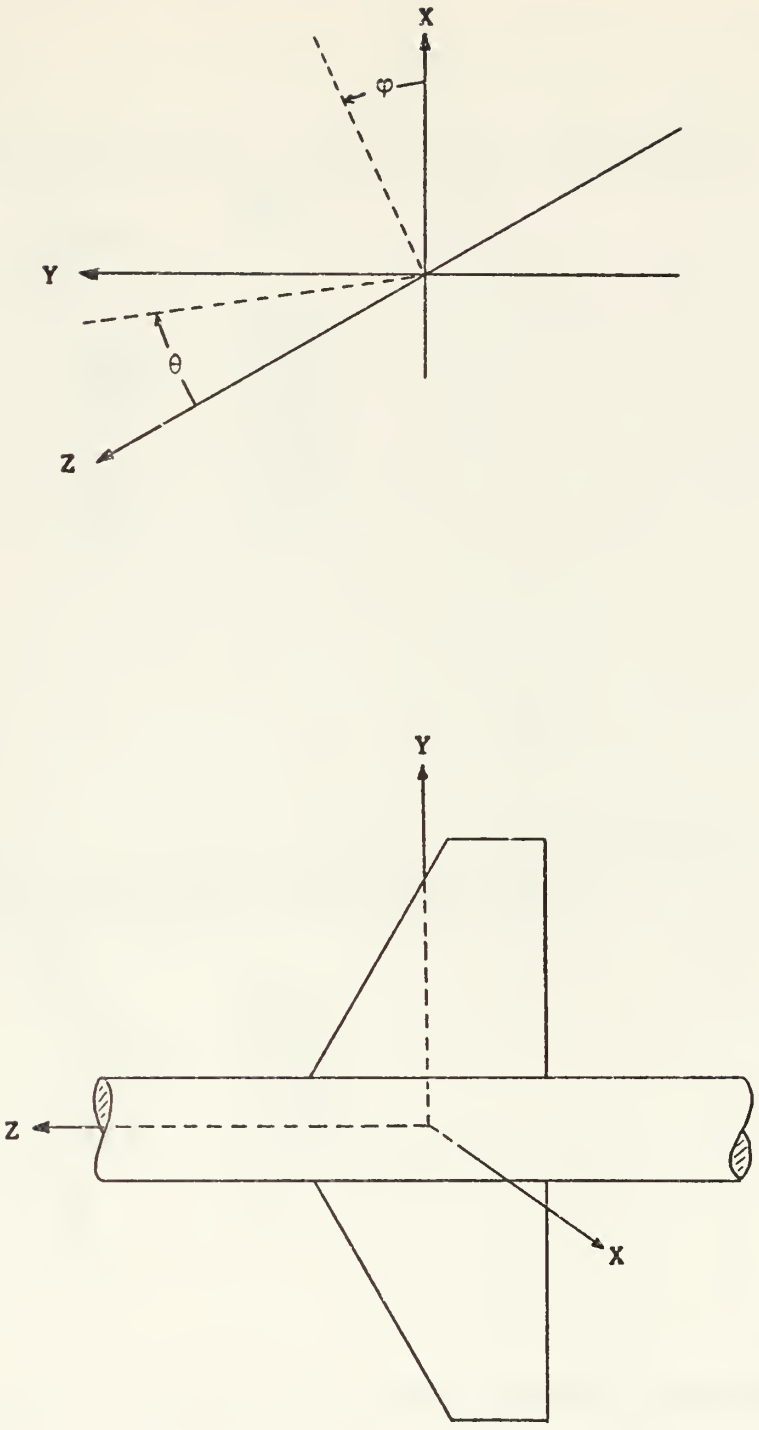

FIG. A-1. COORDINATE SYSTEM USED IN ROLL AND BENT

```
123456789 FOLLOWING IS SAMPLE ROLL INPUT DECK
          2              4.3
36.         36.           0.          0.                    2
TTTTTTTTTTTTTTT
   90    90     1     1
.01          .01
          4              4180.
0.           -36.          59.
0.           -393.7        19.7
0.           -393.7        -19.7
0.           -36.          -59.
          4              4180.
0.           36.           -59.
0.           393.7         -19.7
0.           393.7         19.7
0.           36.           59.
3.            3
```

```
123456789 FOLLOWING IS SAMPLE BENT INPUT DECK
TTTTTTTTTTTTTTTWING FLAT 36INCH FEED
  0    270 90
   90    90     1     1     1
.01          1.0
    6     6.3            180.
0.           0.            59.
0.           -393.7        19.7
0.           -393.7        -19.7
0.           0.            -59.
0.           393.7         -19.7
0.           393.7         19.7
0.           0.
1.           0.
36.          0.            0.
90.          0.
3.            3
```

FIG.A-2. SAMPLE DATA DECKS FOR ROLL AND BENT

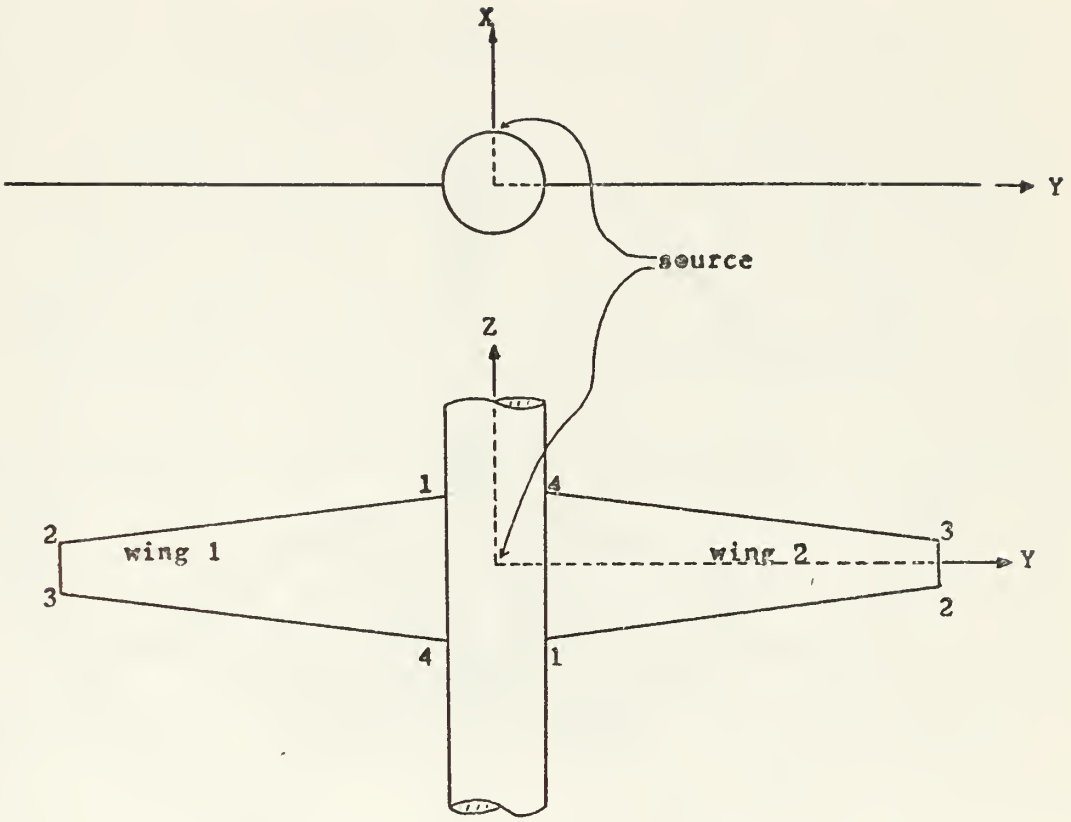

FIG. A-3. SAMPLE PROBLEM GEOMETRY

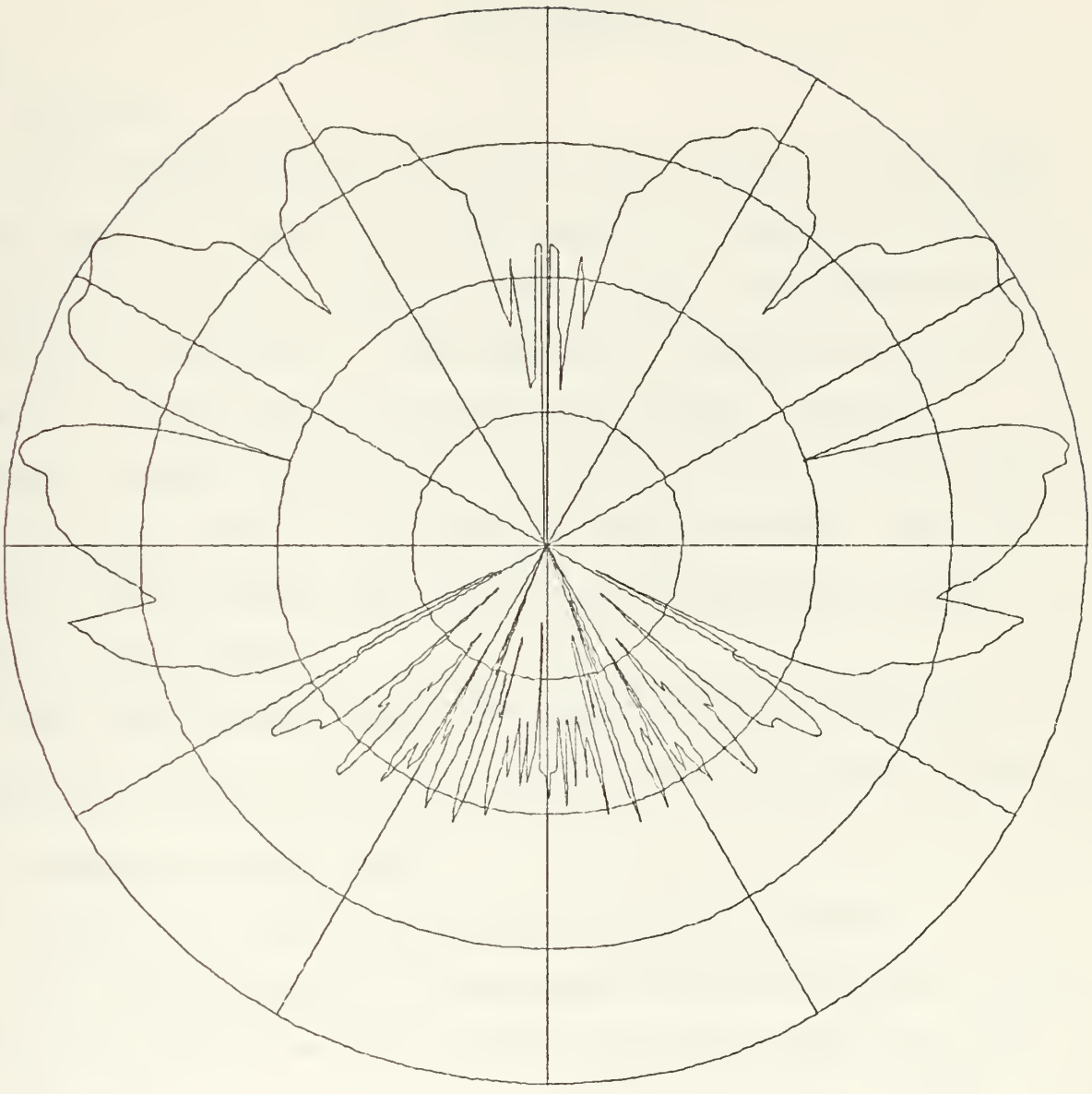

FIG.A-4. ROLL OUTPUT, SAMPLE PROBLEM

II. BENT PROGRAM

A. GENERAL

The OSU BENT program calculates the far field from a flat plate with one bend in it. The fields are calculated from contributions due to direct source energy, reflected energy and diffracted energy. The program is a simplification of the ROLL program only considering one "wing." However, multiple sources (NADC said up to three but the program seems to allow any number -- not checked) may be handled. The program has application when modelling flat fuselage bottoms, wings or tail areas.

The READ (5,9966) RADC, IPLT card (#005120) had to be separated from the call plots card to run on the NPS IBM 360.

B. COMMENTS ON DATA INPUT

Table A-II lists detailed card entries for BENT.

For the orientation in the sample problem, ANGS had to be entered at other than zero so that the final value of E-phi would not be excessive and mis-scale the pen plots. NADC says that RTH equal to 90 will not work. This has not been checked. Small (one lambda or less) plates seem to take excessive run time and produce a size warning in the program.

C. OUTPUT

The POLPLT subroutine required extensive rewriting for compatability with the NPS plot routines. Other output and control are similar to ROLL.

D. GEOMETRY

The coordinate system is as used in ROLL, as shown in Figure A-1.

E. SAMPLE DATA DECK

The sample problem for BENT is just the wing of the ROLL sample problem without the fuselage. The wing is twenty meters in span, three meters at the root, and one meter at the tips. The feed is a dipole directly over the center of the wing thirty-six inches (.914 m) from the wing and oriented perpendicular to the plane of the wing. In other words, the feed is in exactly the same location as on ROLL except the fuselage is missing. The sample data deck is listed in Figure A-3 and polar plot data similar to that for ROLL is in Figure A-5.

TABLE A-II

Input Format for BENT

Card Number	Column Number	Description	Format
1	1-5 6-10 11-15 16-20 21-25 26-35	LWRT = Additional write-out desired (true or false) LPLT = Plot pattern with pen plotter (true or false) LFLAT= Is flat plate considered (true or false) CRAFT= Label for plot, aircraft type PATT = Label for plot, pattern number TYPE = Label for plot, antenna type	3L5, 2A5, A10
2	1-5 6-10 11-15	PT = Label top of plot PL = Label left of plot PR = Label right of plot	3A5
3	1-5 6-10 11-15	THETA and PHI are radiation angles ITHI = Initial value of THETA in degrees ITHF = Final value of THETA in degrees ITHS = Incremental step in THETA IPHS = Incremental step in PHI NUM = Number of sources Note: If ITHI does not equal ITHF, then the three source cards (per source) and the plot size/type card must be reentered for each step. As written, IPHS must equal 1	5I5
4	1-10 11-20	ANGS = Initial value of PHI DELPHI = Incremental value of PHI Note: As written, DELPHI must equal 1.0	2F10.5
5	1-5 6-10 11-20 21-30	MX = Number of corners MC = Number of corner junctions, with bend between corner #1 and MC FRQG = Frequency in gigahertz RTH = Angle of bend in plate, only defined between 90 and 270 degrees Note: If LFLAT is true, then MC=MX and RTH=180. See input discussion	2I5, 2F10.5

TABLE A-II (cont'd)

Card Number	Column Number	Description	Format
6 to 5+MX	1-10 11-20 21-30	Corner locations in inches X coordinate Y coordinate Z coordinate	3F10.5
6+MX	1-10	THC = THETA rotation angle of the axis of pattern rotation PHC = PHI rotation angle of the axis of pattern rotation Note: Angles in degrees. ITHI and ITHF are values in this rotated coordinate system	2F10.5
7+MX	1-10 11-20	The next three cards control the location and orientation of sources. Repeat these cards for each source. ACUR = Amplitude of source PHCUR = Phase of source in degrees	2F10.5
8+MX	1-10 11-20 21-30	Location of source in inches X coordinate Y coordinate Z coordinate	3F10.5
9+MX	1-10 11-20	THOO = THETA rotation angle of source with respect to reference coordinate system PHOO = PHI rotation angle of source	2F10.5
10+MX	1-10 11-12	Use only if LPLT is true RADC = Radius of polar plot on pen plotter in inches. Recommend 3 IPLT = 1 = Field Plot 2 = Power Plot 3 = DB Plot Note: Again, if there are steps in THETA, then the source and plot cards must be repeated for each step.	F10.5, I2

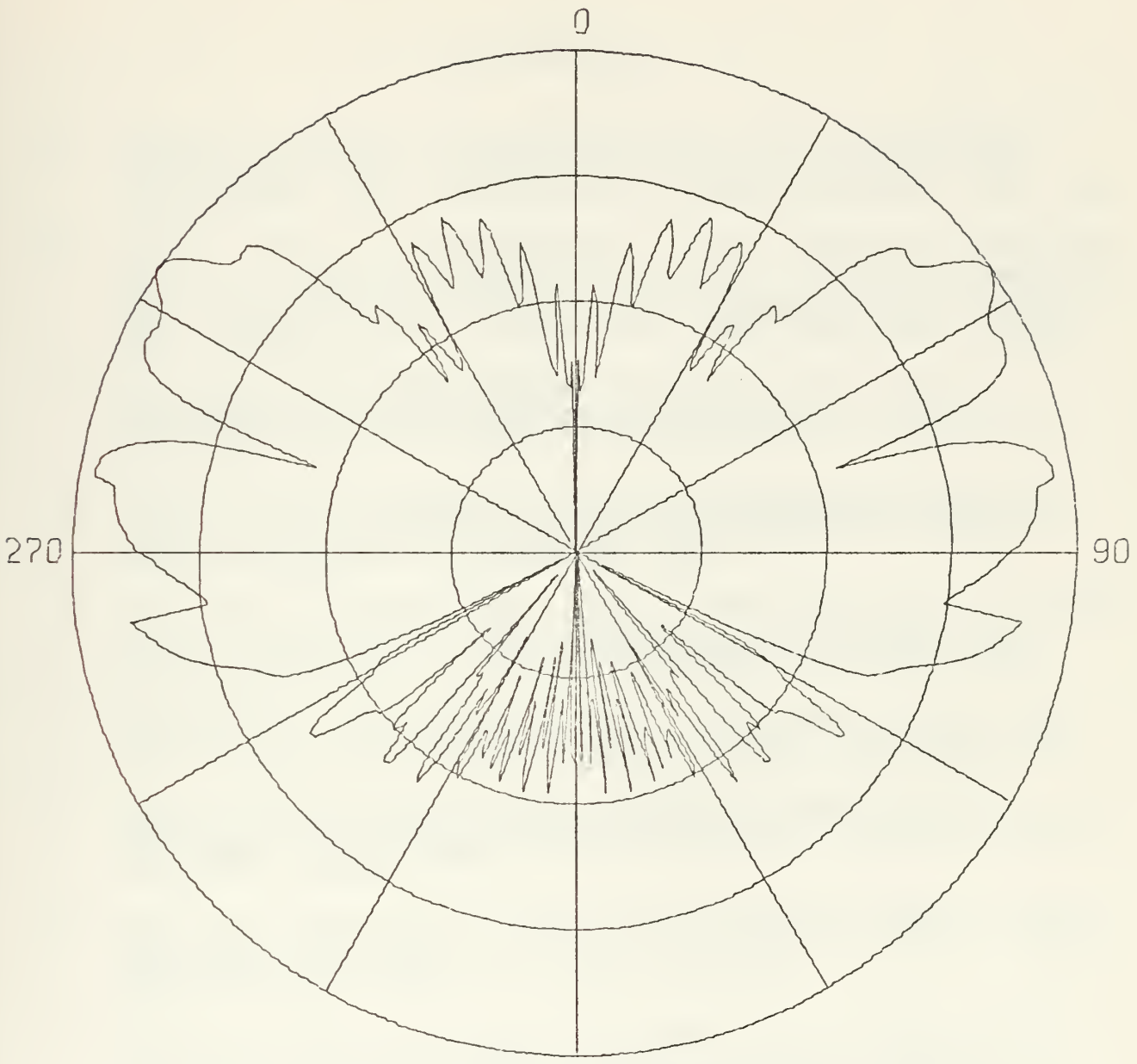

E-PHI DB PLOT 40 DB SCALE
NO. OF CORNERS OF PLATE= 6
ROTATION ANGLE OF PLATE= 180.000
FREQUENCY= 0.300
ANTENNA TYPE= 36INCH FEE
THETA ROTATION ANGLE OF DIPOLE= 90.000
PHI ROTATION ANGLE OF DIPOLE= 0.000
PATTERN NO. FLAT

FIG.A-5. BENT OUTPUT, SAMPLE PROBLEM

BIBLIOGRAPHY

1. Richmond, Jack H., "A Wire-Grid Model for Scattering by Conducting Bodies," IEEE Transactions on Antennas and Propagation, Vol. AP-14, No. 6, November 1966, pp. 782-786.

2. Knepp, Dennis L. and Goldhirsh, Julius, "Numerical Analysis of Electromagnetic Radiation Properties of Smooth Conducting Bodies of Arbitrary Shape," IEEE Transactions on Antennas and Propagation, Vol. AP-20, No. 3, May 1972, pp. 383-388.

3. Royal Aircraft Establishment Technical Report 74077, Computation of the Performance of HF Aerials Mounted On Aircraft, by D. H. Forgan, 10 June 1974.

4. Kubina, S.J., Application Tests of the Antenna Modelling Program (AMP), Concordia University, Montreal, Letter Report EE-74-102, 27 September 1974.

5. Lin, Yau T. and Richmond, Jack H., "EM Modelling of Aircraft at Low Frequencies," IEEE Transactions on Antennas and Propagation, Vol. AP-23, No. 1, January 1975, pp. 53-56.

6. Tanner, R.L. and Anderasen, M.G., "Numerical Solution of Electromagnetic Problems," IEEE Spectrum, September 1967.

7. Naval Air Development Center Technical Report 3390-1, Analysis of On-Aircraft Antenna Patterns, by Walter Dennis Burnside, August 1972.

8. Naval Air Development Center Final Technical Report 3390-2, Analysis of On-Aircraft Antenna Patterns, by Walter Dennis Burnside, May 1973.

9. Thiele, Gary A., and Newhouse, Thomas H., "A Hybrid Technique for Combining Moment Methods with the Geometrical Theory of Diffraction," IEEE Transactions On Antennas and Propagation, Vol. AP-23, No. 1, January 1975, pp. 62-69.

10. Rockway, J.W., Gain and Effective Area of Dipoles and Monopoles, Naval Electronics Laboratory Center, 24 September 1974.

11. MB Associates Information Systems Division of California, Antenna Modelling Program ECOM User's Manual, IS-R-72/11.

INITIAL DISTRIBUTION LIST

		No. Copies
1.	Defense Documentation Center Cameron Station Alexandria, Virginia 22314	2
2.	Library, Code 0212 Naval Postgraduate School Monterey, California 93940	2
3.	Department Chairman (Code 57) Department of Aeronautics Naval Postgraduate School Monterey, California 93940	1
4.	Assoc. Professor S. Jauregui, Jr., Code 52Ja Department of Electrical Engineering Naval Postgraduate School Monterey, California 93940	5
5.	Asst. Professor R. W. Adler, Code 52 Department of Electrical Engineering Naval Postgraduate School Monterey, California 93940	5
6.	Lt. Richard E. Koehler, USN Naval Postgraduate School SMC 2302 Monterey, California 93940	2
7.	Dr. D. Burnside Electroscience Lab Ohio State University 1320 Kinnear Road Columbus, Ohio 43212	1
8.	J. C. P. McEachen Naval Sea Systems Command Code SEA 06T Washington, D.C. 20360	1
9.	Lt. R. B. Birchfield Naval Material Command Code OmAT 034 Washington, D.C. 20360	1
10.	Dr. R. C. Hansen Suite 218 17100 Ventura Blvd Encino, California 91316	1

11. Commander — 2
Naval Security Group Command
3801 Nebraska Avenue, N.W.
Washington, D.C. 20390
Attn: G80
CDR H. Orejuela

12. Naval Electronics Systems Command — 1
Naval Electronics Systems Command Headquarters
Washington, D.C. 20360
Attn: PME 107
LCDR R. Shields

13. Director — 1
National Security Agency
Fort Meade, Maryland
Attn: R. Group - Mr. C. B. Kelley

14. Naval Electronics Systems Command — 1
Naval Electronics Systems Command Headquarters
Washington, D.C. 20360
Attn: PME 107
LCDR A. Sagerian

15. Naval Electronics Laboratory Center — 1
271 Catalina Blvd.
San Diego, California 92152
Attn: LT W. Gadino

16. Naval Electronics Systems Command — 1
Naval Electronics Systems Command Headquarters
Washington, D.C. 20360
Attn: PME 107
Mr. William Claussan

17. Russel M. Brown — 1
Code 5252
Naval Research Laboratory
Washington, D.C. 20390

18. John A. Downs — 1
Code 3556
Naval Weapons Center
China Lake, California 93555

19. Dennis E. Fessenden — 1
Code SA32
Naval Underwater Systems Center
New London, Conn. 06320

20. Major Anthony Martinez — 1
(LZR)
Air Force Communications Research Laboratory
Hanscom Field, Mass. 01730

21. Dr. E. K. Miller (L158) — 1
Lawrence Livermore Laboratory
P.O. Box 808
Livermore, Calif. 94550

22. Dr. John W. Rockway — 1
Naval Electronics Laboratory Center
Code 2120
San Diego, Calif. 92152

23. Al Mink, Code 6179 — 1
Naval Ships Engineering Center
Hyattsville, Md. 20784

24. Fran Prout, Code 6174 — 1
Naval Ships Engineering Center
Hyattsville, Md. 20784

25. Tony Testa, Code 6174 — 1
Naval Ships Engineering Center
Hyattsville, Md. 20784

26. Dr. S. Siahatgar, Code 6174 — 1
Naval Ships Engineering Center
Hyattsville, Md. 20784

27. Dr. A. Sankar — 1
MS R-1 1144
TRW Systems, 1 Space Pack
Redondo Beach, Calif. 90278

28. Ronald Prehoda — 1
Code FVR
Naval Surface Weapons Center
Dahlgren, Va. 22448

29. CDR E. G. Neely, III — 1
Naval Electronics Systems Command
Code ELEX 094
Washington, D.C. 20360

30. Dr. R. Tanner — 1
Technology for Communication International
1625 Stierlin Road
Mt. View, Calif. 94043

31. Dr. B. Strait — 1
Electrical Engineering Department
111 Link Hall
Syracuse University
Syracuse, NY 13210

32. Walter Curtis 1
Boeing Aerospace Co.
P.O. Box 3999
Seattle, Wash. 98124

33. Dr. Raj Mittra 1
Electrical Engineering Department
University of Illinois
Urbana, Ill. 61801

34. CDR Russ Shields 1
Naval Electronics System Command
Code PME-107
Washington, D.C. 20360

35. Mr. Bob Lee 1
Code 2041
Naval Air Development Center
Warminster, Pa. 18974

36. Mr. Keith Struckman 1
Sanders Associates, Inc.
95 Canal Street
Nashua, N.H. 03060